Through-Wall Imaging Radar

John E. Peabody, Jr., Gregory L. Charvat, Justin Goodwin, and Martin Tobias

The ability to locate moving targets inside a building with a sensor situated at a standoff range outside the building would greatly improve situational awareness on the urban battlefield. A radar imaging system was developed to image through walls, providing a down-range versus cross-range image of all moving targets at a video frame rate. This system uses an S-band, frequency-modulated, continuous-wave radar with a spatial frequency range gate coupled to a time-division multiplexed, multiple-input, multiple-output antenna array to rapidly acquire, process, and display radar imagery at a frame rate of 10.8 Hz. Maximum expected range through a 20 cm thick, solid concrete wall is 20 m. Measurements show that this system can locate humans (moving or standing still) behind 10 and 20 cm thick, solid concrete walls and through "cinder-block" walls.

Knock and announce missions occur frequently on the urban battlefield. It would be advantageous to locate all of the humans inside an urban structure and obtain a "head count" prior to action. For this reason, we developed a through-wall radar sensor capable of locating moving targets through concrete-walled structures and of displaying the results (in range versus cross range) at a video frame rate of 10.8 Hz while the sensor is a safe distance from the wall. This sensor, approximately 2.25 m in length, would be mounted to a vehicle and driven near a building at a standoff range from which the user may detect the moving targets inside the building, as shown in Figure 1.

The sensor uses a frequency-modulated, continuous-wave (FMCW) radar architecture operating at S-band, where some wall penetration is possible, with a center frequency of 3 GHz with a 2 GHz ultrawideband chirp. A narrowband, spatial frequency filter provides a range gate that eliminates the wall from the image, facilitating maximum receiver dynamic range to be applied to the target scene behind the wall. A time-division multiplexed (TDM), multiple-input, multiple-output (MIMO) array provides a lowest-cost, least complicated solution to a fully populated antenna aperture capable of near-field imaging. To achieve video-frame-rate imaging, a data pipeline and streamlined imaging algorithm were developed. Coherent frame-to-frame processing rejects stationary clutter, revealing the location of moving targets.

In previous work, the switched-antenna-array, through-wall radar sensor was shown to be effective at imaging human targets through a 10 cm thick, solid concrete wall at a 6 m standoff range at the rate of one image

every 1.9 seconds [1, 2]. The imaging algorithm is a real-time implementation of the range migration algorithm (RMA) synthetic aperture radar (SAR) imaging algorithm based on work from a high-speed imaging architecture originally developed for real-time interferometric synthetic aperture microscopy [3].

For the system shown in this article, the maximum range when imaging through a 20 cm thick, solid concrete wall is estimated to be 20 m. Free-space measurements will show that this system is capable of resolving rapidly moving human targets and low radar-cross-section (RCS) targets. Through-wall measurements will show that this system is capable of locating human targets that are either moving or standing still behind 10 cm and 20 cm thick, solid concrete walls and through cinder-block walls at a standoff range approximately 6 m from the wall and 10 m from the targets. Preliminary detection work demonstrates the feasibility of plotting detections and providing a head count in real time rather than displaying raw SAR imagery. Future work will include testing on an adobe structure and actual random buildings with diverse target scenes.

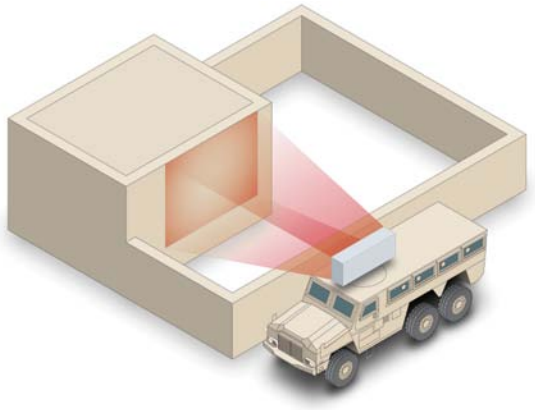

FIGURE 1. The through-wall radar sensor would be mounted on a vehicle and would operate at standoff ranges, providing range and cross-range position of moving targets within an urban structure.

System Description

The radar system can be described in four parts: the hardware, the antenna array, the imaging algorithm, and the data acquisition and graphical user interface (GUI). Photographs of the radar system are shown in Figure 2.

Radar System

The core of this system is a range-gated FMCW radar device that transmits linear frequency-modulated (LFM) chirps from 2–4 GHz in 1 ms with 1 W peak transmit power at 50% duty cycle. Figure 3 shows the transmit and receive ports are fed to fan-out switch matrices connected to the array elements. This radar architecture implements a range gate by using a high-Q intermediate-frequency (IF) filter FL1 [4]. This filter band-limits the decorrelated LFM prior to pulse compression, resulting in an effective range gate of the target by rejecting scattered returns from the air-wall boundary, thereby providing a spatial frequency range gate. This design provides maximum dynamic range and sensitivity for imaging targets behind a wall [5, 6].

Antenna Array

The antenna array is shown in Figure 2a. The transmit port of the FMCW radar is connected to a fan-out switch matrix made up of switches SW1–3 (shown in Fig-

(a)

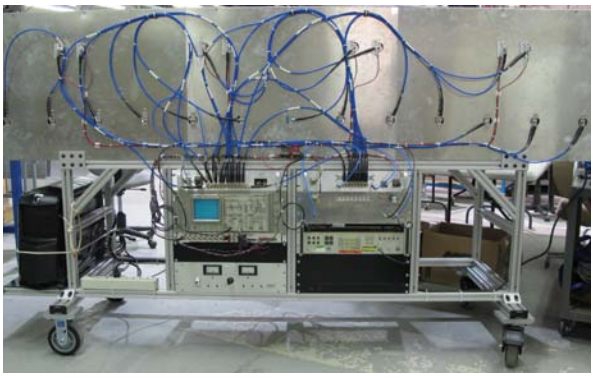

(b)

FIGURE 2. Photographs of the through-wall radar imaging system show (a) the antenna elements on the front of the system, and (b) the transmitter, receiver, power supplies, diagnostic oscilloscope, and computer on the back.

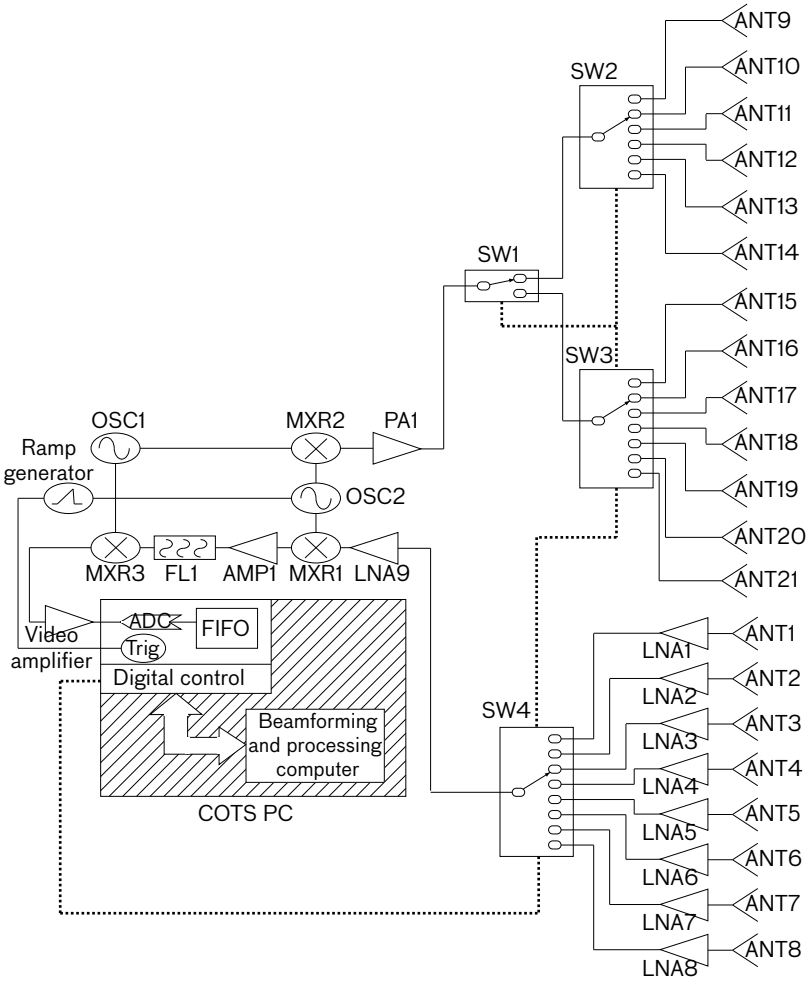

FIGURE 3. The radar block diagram depicts the range-gated, frequency-modulated, continuous-wave (FMCW) system, which facilitates through-wall imaging, connected to receive and transmit fan-out switch matrices that feed all antenna array elements.

ure 3) where the transmit port is fed to only one antenna element (ANT9–21) at a time. Similarly, the receive port of the radar system is connected to an eight-port switch (SW4) that connects to one low-noise amplifier (LNA1–8) at a time. Each LNA is connected to and physically mounted to a receiver element (ANT1–8) to preserve the noise figure through feed line and system losses.

The antenna element (the top layer is shown in Figure 4) is based on a combination of a Vivaldi and linear tapered-slot design and is capable of supporting at least 2–4 GHz of bandwidth with efficient radiation and useful E and H plane beamwidths.

The radar uses only a subset of all possible antenna combinations, which consist of 44 bistatic antenna element combinations whose effective phase centers approximate a linear array evenly spaced $\lambda/2$ [2]. These bistatic antenna combinations are shown in Figure 5; the large circles represent ANT1–21, the lines represent the bistatic baselines, and the small circles represent the effective phase centers.

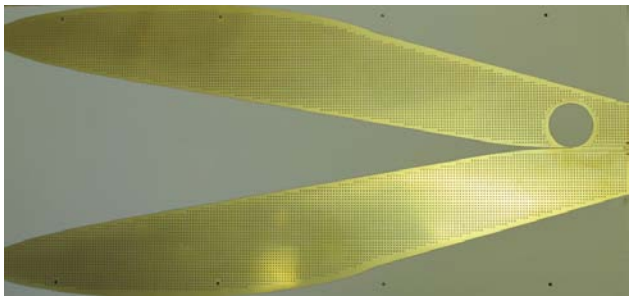

FIGURE 4. A single hybrid antenna using a combination of a Vivaldi and linear slot design is shown. An array of these populates the through-wall radar system.

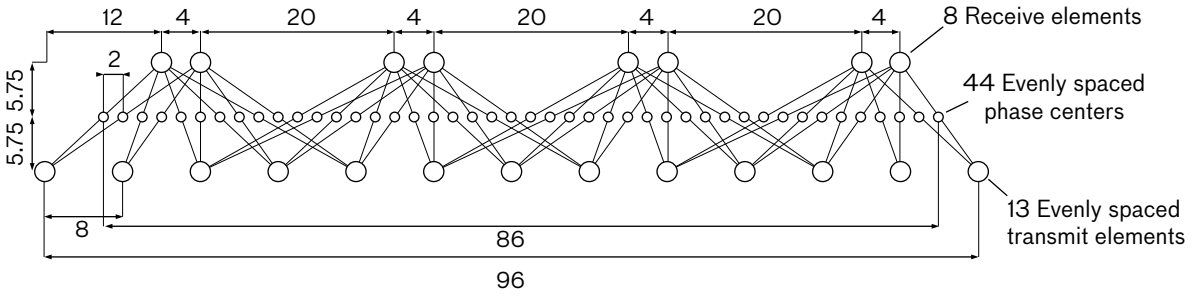

FIGURE 5. In this cartoon of the time-division multiplexed (TDM), multiple-input, multiple-output (MIMO) array layout [compare to Figure 2(a)](units in inches), large circles represent the antenna elements. The lines between the elements show the bistatic baselines, and the smaller circles indicate the location of each phase center. With this array, 44 virtual elements can be synthesized with just 21 actual antenna elements.

All antenna switches (SW1–4) are solid state and digitally controlled by the data-acquisition computer. The TDM MIMO radar system sequences through each of the 44 bistatic combinations, acquiring one range profile at each. The computer controls the switches, pulses the transmitter, and digitizes the video; executes these tasks in a continuous loop; and simultaneously computes and displays a SAR image at a rate of 10.8 Hz.

Imaging Algorithm

This radar resolves targets by using the RMA, which is a near-field SAR imaging algorithm [7]. Processing a single image with the RMA is computationally expensive. A careful implementation of the RMA was developed so that values are precomputed and preorganized in the memory whenever possible. A real-time beamforming algorithm in a C++ class was designed to execute a high-speed, hardware-optimized RMA. A MATLAB executable (MEX) interface was designed to prototype the algorithm in a debug environment. This interface allows for continued development of processing routines. The combination of these streamlined processes provides real-time imaging at a rate of 10.8 Hz [5].

Data Acquisition and Graphical User Interface

The data-acquisition (DAQ) system acquires data from the radar and provides system control through a GUI that displays the processed data and establishes a pipeline to and from the data processing algorithms to facilitate real-time radar imaging frame rates. A block diagram of the DAQ system is shown in Figure 6. A screen shot of the GUI is shown in Figure 7 [5].

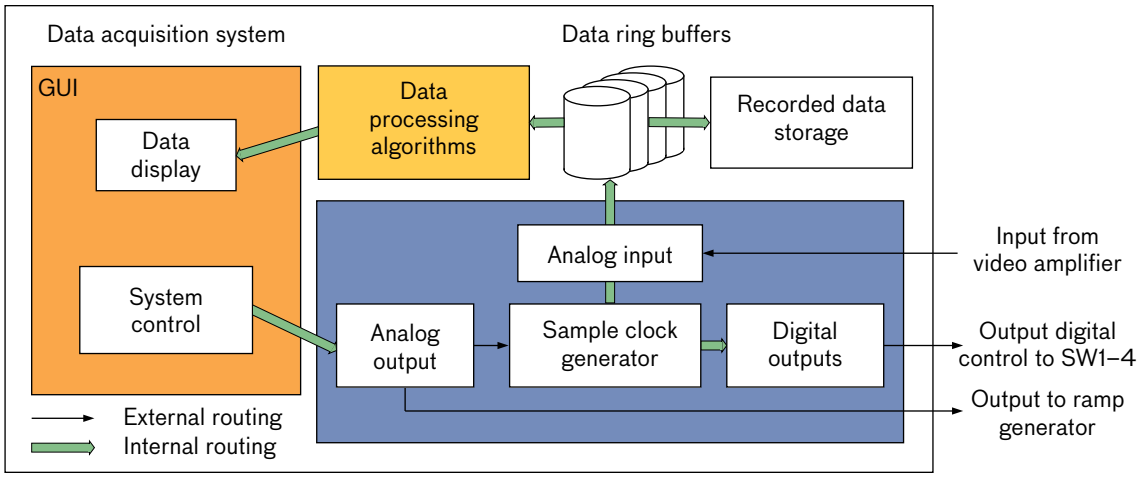

FIGURE 6. The data acquisition (DAQ) system facilitates real-time imaging by using a high-speed data pipeline and real-time implementation of a synthetic aperture radar (SAR) imaging algorithm.

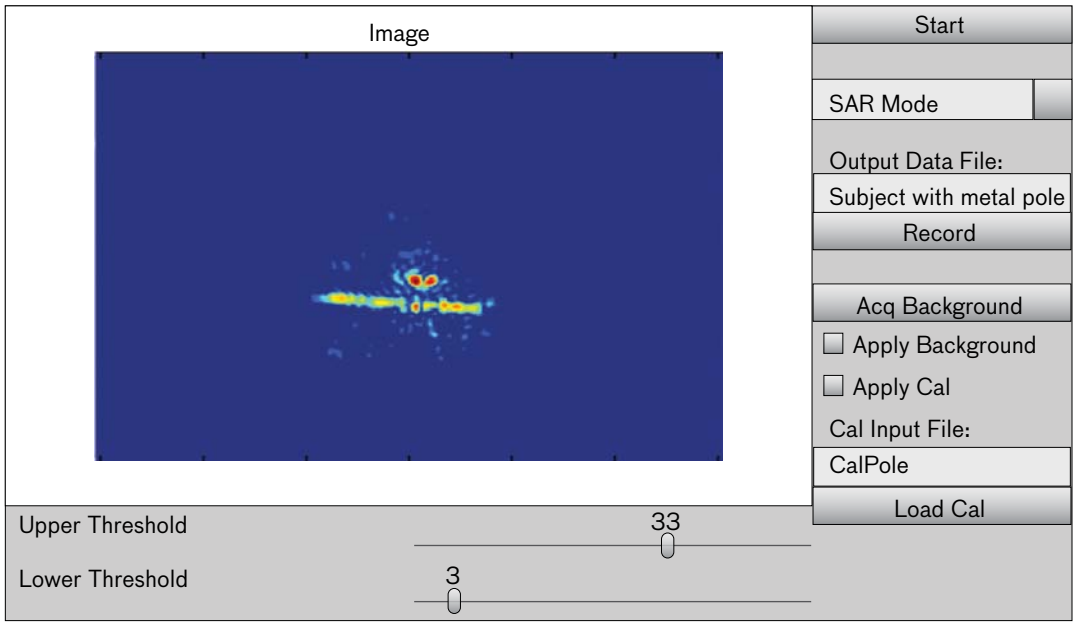

FIGURE 7. The graphical user interface has controls for starting the radar, imaging mode, output file name, record (on or off), record background, apply background, apply calibration, calibration input file name, load calibration, and dynamic range vernier sliders for both the upper and lower threshold.

System Model

A thermal-noise-limited, maximum-range model was developed by inputting the antenna gain estimate and the array factor into the radar range equation [6]. Although this model only accounts for thermal-noise-limited performance, it shows the potential for this technology in a through-wall application.

In this model, the two-way wall attenuation was accounted for as a loss factor. Range resolution was estimated for every pixel inside of the radar field of view, where the single-image, signal-to-noise ratio (SNR) was greater than 13.66 dB. Figure 8 illustrates the return intensities expected for a human target (0 dBsm) through a 20 cm thick, solid concrete wall with a two-way loss of 90 dB [8]. On the basis of these calculations, the estimated maximum range is 20 m with a down-range resolution of 7.5 cm and a worst-case, cross-range resolution of 45 cm. At ranges less than 20 m, cross-range resolution is better than 45 cm.

Results

Radar imagery was acquired at an imaging rate of 10.8 Hz. The system was demonstrated on rapidly moving targets in free space, humans behind concrete walls, and humans standing still behind concrete walls.

Free-Space Imagery

To show that this radar is capable of imaging in a high-clutter environment with rapid target movements, a person swinging a metal rod was imaged in front of the radar about 5 m away and centered with respect to the array in free space. Range gating and frame-to-frame coherent change detection were used to eliminate clutter. Each data set was coherently subtracted from the previous one. Continuous, coherent, change detection of the target scene

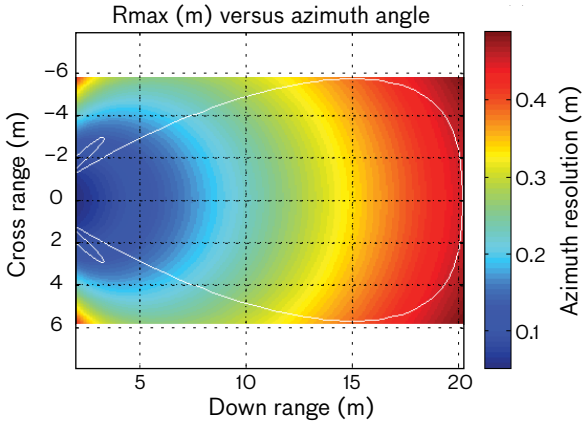

FIGURE 8. Estimated maximum range for imaging through a 20.3 cm thick, solid concrete wall. The white line indicates the maximum detection range for a 0 dBsm target with an SNR greater than 13.66 dB.

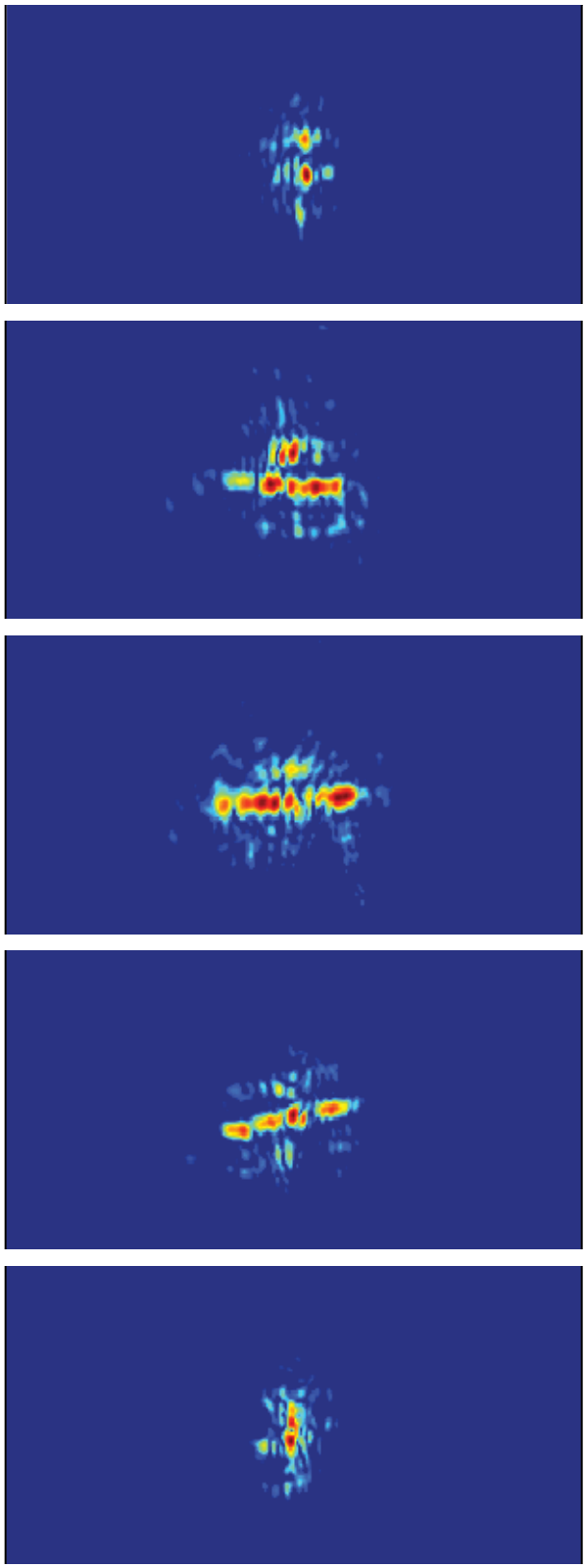

FIGURE 9. The metal rod being rotated by a human is clearly visible in these images. The imagery is in range vs. cross range with 20 dB of dynamic range shown.

clearly shows the range versus cross-range imagery of a human target and the specular reflection of the rotating metal rod without noticeable blurring (every other frame is shown in Figure 9).

Coherent background subtraction was used to image a pair of metal spheres with diameters of 2.5 cm located approximately 4 m down range from the array. One sphere remains stationary and the other rolls past, as shown in Figure 10. Multipath scattering from the spheres is noticeable as one sphere passes close to the other. The RCS of a 2.54 cm diameter sphere at the radar center frequency of 3 GHz is approximately −29 dBsm. The clear radar images of the stationary and moving spheres demonstrate the sensitivity of this real-time radar sensor.

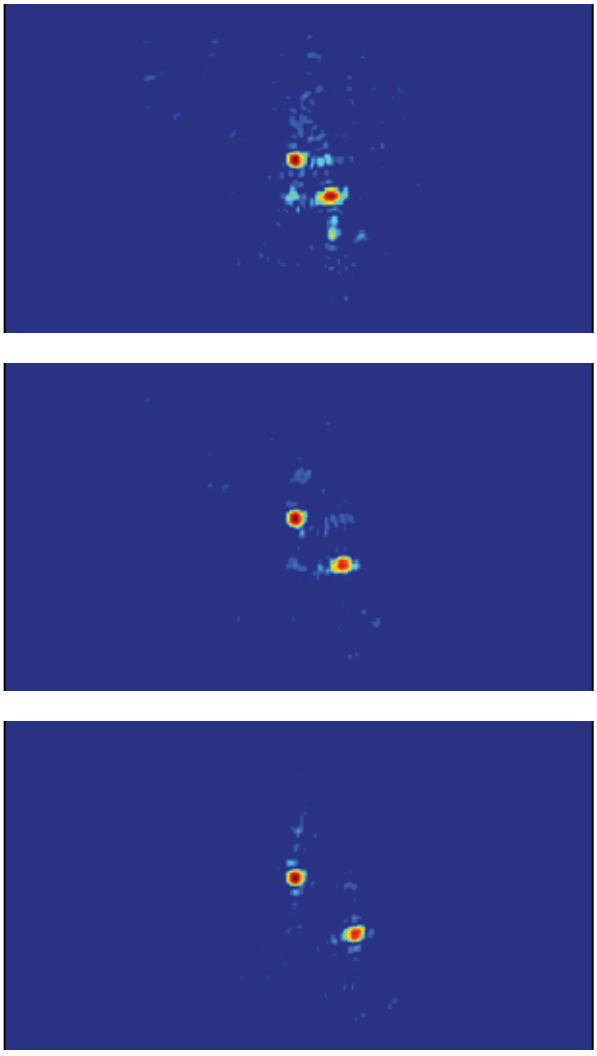

FIGURE 10. Here, one 2.5 cm diameter metal sphere is rolled past another in real time. The imagery is in range vs. cross range with 20 dB of dynamic range shown.

FIGURE 11. The "test range" for through-wall measurements shows the 10 cm and 20 cm thick, solid concrete walls on the left and the cinder-block wall on the right.

Through-Wall Imagery

Through-wall imagery of two humans behind three types of walls and in free space (for reference) were acquired. Although the radar acquires data in real time, only one image frame is shown for each result. The walls, shown in Figure 11, were purpose-built for radar testing and included 10 cm and 20 cm thick, solid concrete walls and a cinder-block wall. The through-wall imaging geometry is shown in Figure 12. The radar is approximately 6 m standoff distance from the wall, and the humans are approximately 10 m from the radar behind the wall. The reference image in Figure 13 shows what two humans look like on the radar screen without a wall present. Down-range sidelobes are as expected, and cross-range sidelobes are elevated.

Two humans were imaged through 10 cm and 20 cm thick, solid concrete walls and a cinder-block wall (Figure 14). In each scenario, the signal-to-clutter ratio is sufficiently large to facilitate detection.

- Humans behind the 10 cm thick wall (Figure 14a) appear similar to humans in free space, and their locations are clearly shown with a good signal-to-clutter ratio.
- Humans behind the 20 cm (Figure 14b) thick wall have a significantly lower scattered return. There appears to be more clutter, which is likely receiver noise, but each human's location is clearly shown and their relative magnitudes are greater than 15 dB above the clutter floor.
- Human images viewed through the cinder-block wall (Figure 14c) appear to be strong but so is the clutter. This result is likely due to the air gaps within the cinder blocks, which cause additional propagation-path distortion.

In at least half of the experiments imaged in real time, the location of each human is clear relative to the clutter. With the application of detection and tracking algorithms, it should be possible to provide a reliable detection.

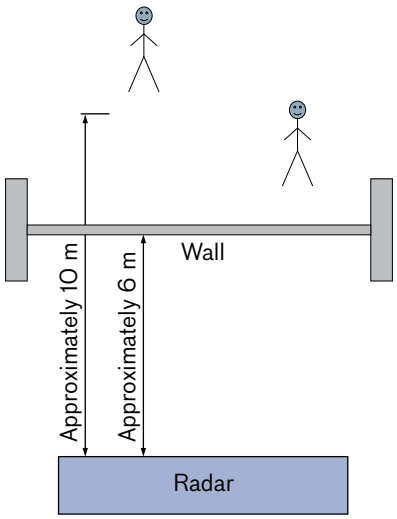

FIGURE 12. This cartoon of the geometry of the through-wall imaging measurements shows two individuals behind the barrier wall.

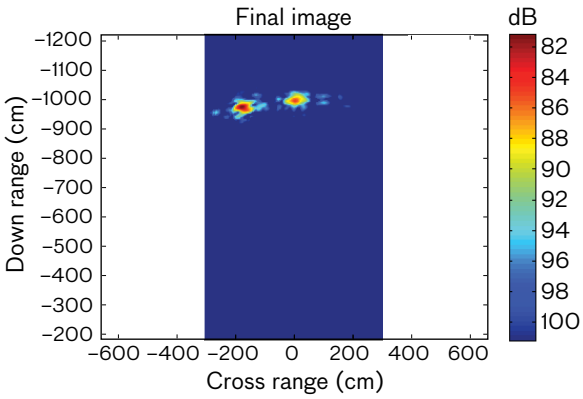

FIGURE 13. For reference purposes for the following through-wall experiments, this is an image of two humans in free space (no wall).

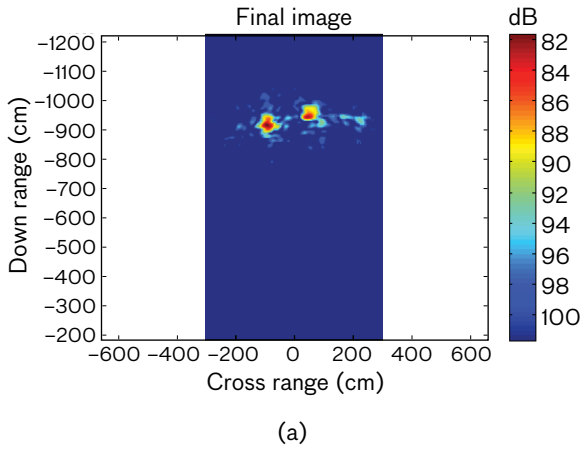

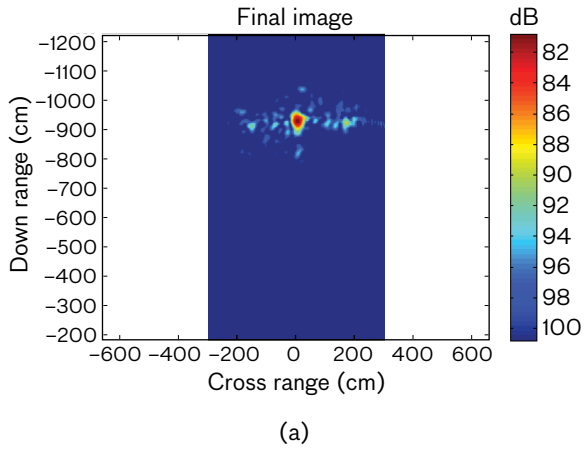

FIGURE 14. Two humans are imaged through a 10 cm thick, solid concrete wall (a), through a 20 cm thick, solid concrete wall (b), and through a cinder-block wall (c).

FIGURE 15. A single human standing still can still be easily detected behind a 10 cm, solid concrete wall (a), behind a 20 cm, solid concrete wall (b), and behind a cinder-block wall (c).

Wall type	One walking	Two walking	Standing still	Sitting still	Standing still holding breath	Sitting still holding breath
20 cm concrete						
Cinder block						
10 cm concrete						
Free space						

Through-Wall Imagery of Humans Standing Still

Even when standing still, a human could be detected through the concrete walls because the human body moves slightly when breathing and while trying to remain upright. Results for one human standing still behind 10 cm and 20 cm thick, solid concrete walls and a cinder-block wall are shown in Figure 15. The location of the human behind the 10 cm thick, solid concrete wall was clearly observed (Figure 15a). Similarly, the location of the human target through the cinder-block wall was clearly visible (Figure 15c) with a slight increase in clutter, probably caused by air gaps within the blocks.

To reveal the location of the human behind the 20 cm thick, solid concrete wall, the frame-to-frame, coherent, change-detection algorithm had to subtract from the tenth frame back. The person's location is clearly shown after this analysis was applied (Figure 15b). For cases in which there is a weak return, an adaptive, frame-to-frame, coherent subtraction algorithm that can decide if it is necessary to coherently subtract from one to many frames back should be developed.

Performance Summary

A number of through-wall scenarios were tested and compared to the same scenario in free space. Results are summarized in Table 1. Green, yellow, and red indicate that the target is detectable in the vast majority of image frames, approximately half of the image frames, or none of the image frames, respectively. This table shows that a human target is detectable in all scenarios in free space. When the radar images through a 10 cm thick, solid concrete wall, human targets can be located even if they are standing still and holding their breath but not while sitting still and holding their breath. In the case of the cinder-block wall, human targets can be detected if standing still and holding their breath but not sitting still and holding their breath. Detection and location are sometimes difficult when two humans are walking because of the elevated clutter induced by air gaps in the blocks. A marginal image also occurs when the human is sitting still. Behind the 20 cm thick, solid concrete wall, a human can be detected only if he/she is walking around. The same human can be detected sometimes when standing still, but not standing still and holding his/her breath.

In summary, this radar sensor can locate human targets most of the time through 10 cm and 20 cm thick, solid concrete and cinder-block walls even if the people are standing still but not if they are sitting or holding their breath.

Detection Algorithm

Although radar imagery, as shown in this paper, may provide actionable information to a radar engineer, the field operator prefers to view discrete detections rather than blobs on a radar screen. A radar display that provides detections is valuable because it reduces the observer/analyst training time and generally simplifies decision making. The signal-to-clutter ratio and the point-spread function for most through-wall imagery shown here is sufficient to merit the application of a detection algorithm, with the objective of locating and counting the individual moving targets behind the wall.

A clustering technique that combines detections in adjacent range and cross-range bins into a single human detection is used to detect the number of humans present in an image. The number of bins that are clustered is chosen to correspond to the approximate size expected from a radar return on a human.

Figure 16a shows the radar image of a scene containing two people. Figure 16b shows the range and cross-range bins that exceeded our detection threshold, which we set to 15 dB below the peak SNR in the image. Figure 16c shows the result of clustering the detections, using a + to mark the center of each human detection.

In order to maintain an estimate of the number of humans in a scene over time, we are currently performing

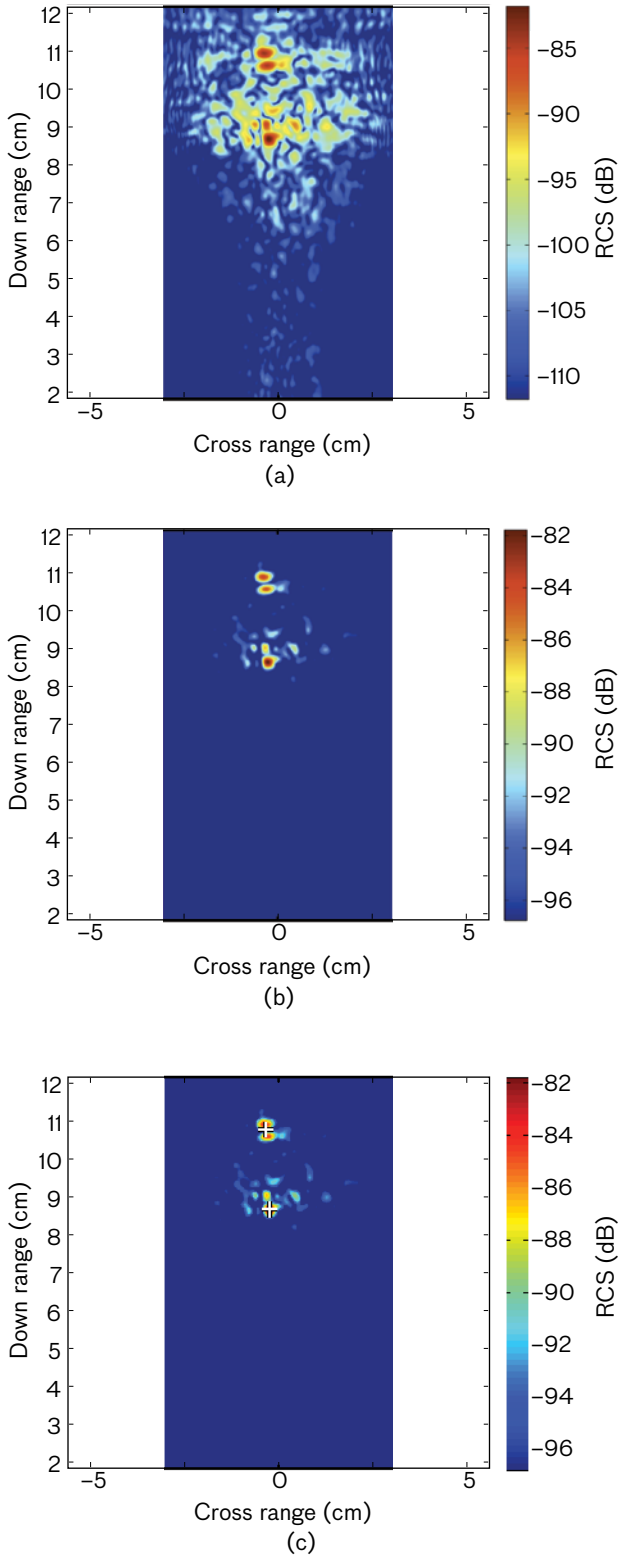

FIGURE 16. The raw data of a through-wall scene containing two humans are shown in (a), when range and cross-range bins exceeding detection threshold are selected (b), and the result of clustering detections into individual detections, which are marked with a + (c).

research on the Gaussian-mixture probability hypothesis density (GM-PHD) [9] filter to form tracks on the human detections. The GM-PHD will aid rejection of spurious detections caused by radar calibration error and false-alarm detections. The filter will provide a running estimate of the number of humans detected. Alternatively, an M of N type of detection scheme, whereby we average the number of detections found over a given number of radar images, may also provide an adequate estimate of the number of humans in the scene. This is currently under investigation.

Next Steps

The next steps are to test this system on an adobe mud-brick wall and to complete development of a detection algorithm. If these steps are successful, this radar will be tested on walls of an actual building. Results of those tests may lead to fielding a prototype. Other applications for which the through-wall system may be used include real-time radar imaging of natural phenomenon or high-speed radar cross-section measurements.

Acknowledgments

The authors would like to acknowledge Tyler S. Ralston, a former Lincoln Laboratory staff member now at Lawrence Livermore National Laboratory, for developing the real-time imaging algorithm, John Sandora for developing the antenna element, and Chao Liu for helping set up the outdoor measurements. ■

References

1. G.L. Charvat, "A Low-Power Radar Imaging System," PhD dissertation, Department of Electrical and Computer Engineering, Michigan State University, East Lansing, Michigan, Aug. 2007.
2. G.L. Charvat, L.C. Kempel, E.J. Rothwell, C. Coleman, and E.J. Mokole, "An Ultrawideband (UWB) Switched-Antenna-Array Radar Imaging System," *Proceedings of the IEEE International Symposium on Phased Array Systems and Technology,* 2010.
3. T.S. Ralston, D.L. Marks, P.S. Carney, and S.A. Boppart, "Real-Time Interferometric Synthetic Aperture Microscopy," *Optics Express,* vol. 16, no. 4, pp. 2555–2569, 2008.
4. G.L. Charvat, L.C. Kempel, E.J. Rothwell, C. Coleman, and E.L. Mokole, "A Through-Dielectric Radar Imaging System," *IEEE Transactions on Antennas and Propagation,* vol. 58, no. 8, pp. 2594–2603, 2010.
5. T.S. Ralston, G.L. Charvat, and J.E. Peabody, "Real-Time Through-Wall Imaging using an Ultrawideband Multiple-Input Multiple-Output (MIMO) Phased-Array Radar System," *Proceedings of the IEEE International Symposium on Phased Array Systems and Technology,* pp. 551–558, 2010.
6. G.L. Charvat, T.S. Ralston, and J.E. Peabody, "A Through-Wall Real-Time MIMO Radar Sensor for Use at Stand-off Ranges," *MSS Tri-Services Radar Symposium,* Orlando, Florida, 2010.
7. W.G. Carrara, R.S. Goodman, and R.M. Majewski, *Spotlight Synthetic Aperture Radar Signal Processing Algorithms.* Boston: Artech House, 1995.
8. P.R. Hirschler-Marchand, "Penetration Losses in Construction Materials and Buildings," MIT Lincoln Laboratory Project Report TR-ACC-1, Rev. 1, 19 July 2006.
9. B.N. Vo and W.K. Ma, "The Gaussian Mixture Probability Hypothesis Density Filter," *IEEE Transactions on Signal Processing,* vol. 54, no. 11, pp. 4091–4101, 2006.

John Peabody Jr. is an assistant staff member in the Aerospace Sensor Technology Group. While attending Wentworth Institute of Technology, where he majored in computer engineering, Peabody accepted an intern position at Lincoln Laboratory in the Aerospace Division. Upon graduation, he accepted a full-time position in the Laboratory. Peabody completed the Master of Science in Information Technology—Software Engineering distance-learning program from Carnegie Mellon University in 2011. He is currently the Massachusetts Affiliate Partner for the For Inspiration and Recognition of Science and Technology (FIRST) Tech Challenge.

Gregory Charvat is currently the co-founder and research engineer at Butterfly Networks, Inc. In graduate school, Charvat developed rail SAR imaging sensors, a MIMO phased-array radar system, and an impulse radar. He holds a patent on a harmonic radar remote sensing system. While a member of the technical staff at Lincoln Laboratory, he developed a MIMO through-wall radar system. He has also taught several short courses on radar at MIT and authored numerous articles in journals and IEEE proceedings. Charvat received his bachelor's and master's (in electrical engineering) and doctorate (in 2007) degrees from Michigan State University. He is a Senior Member of the IEEE. He served on the 2010 and will serve on the 2013 IEEE Symposia on Phased Array Systems and Technology steering committees and chaired the IEEE Antennas and Propagation Society Boston Chapter from 2010–2011.

Justin Goodwin is a member of the technical staff at Lincoln Laboratory. Since joining the Laboratory in 2002, his focus has been on the development of algorithms and architectures to support ballistic missile defense sensors in the areas of tracking and discrimination. Goodwin received a bachelor's degree in mathematics from the University of Puget Sound, and bachelor's and master's degrees in systems science engineering from Washington University.

Martin Tobias is a technical staff member in the Systems and Architectures Group. He received his bachelor's degree summa cum laude from Harvard University in 1999 and spent a few years working at Internet hardware startup companies. He joined Lincoln Laboratory in 2006 after receiving his master's and doctorate degrees from the School of Electrical and Computer Engineering at the Georgia Institute of Technology, where his research focused on multitarget, multisensor tracking.